Variable Parameter Sliding Controller Design for Vehicle Brake with Wheel Slip

Hong Liang, Kil To Chong*

Faculty of Electronics and Information, Chonbuk National University, Duckjin-Dong, Duckjin-Gu, Chonju, 561-756, South Korea

In this paper, a 4-wheel vehicle model including the effects of tire slip was considered, along with variable parameter sliding control, pushrod force as the end control parameter, and an antilock sliding control, in order to improve the performance of the vehicle longitudinal response. The variable sliding parameter is made to be proportional to the square root of the pressure derivative at the wheel, in order to compensate for large pressure changes in the brake cylinder. A typical tire force-relative slip curve for dry road conditions was used to generate an analytical tire force-relative slip function, and an antilock sliding control process based on the analytical tire force-relative slip function was used. A retrofitted brake system, with the pushrod force as the end control parameter, was employed, and an average decay function was used to suppress the simulation oscillations. Simulation results indicate that the velocity and spacing errors were slightly larger than the results that without considering wheel slip effect, the spacing errors of the lead and follower were insensitive to the adhesion coefficient up to the critical wheel slip value, and the limit for the antilock control on non-constant adhesion road condition was determined by the minimum of the equivalent adhesion coefficient.

Key Words : Automatic Highway Vehicles, Wheel Slip, Antilock Control, Sliding Control, Variable Parameter, Smoothing

1. Introduction

With rising public concern about transportation issues such as roadway capacity, traffic congestion and highway safety, interest in Intelligent Vehicle Highway Systems (IVHS) has never been greater. Among the proposed systems, much attention has been focused on the use of Advanced Vehicle Control Systems (AVCS) to produce lanes of automated vehicles traveling in closely spaced platoons. The design of integrated control between throttle and brake is an important subject in the research of AVCS (Utkin, 1997; Lee and Park, 1999; Haskara et al., 2000; Choi and Hederick, 1996). Swaroop (1994) used a second-order model including throttle control and braking without delays to design a linear controller. An improved technique was proposed by Chien et al. (1994) to further consider safety problems. Maciuca and Hedrick (1995) introduced an advanced nonlinear sliding brake control. Huang and Ren (1999) introduced a learning switch algorithm with a zero control delay time for the switching between throttle and brake. Choi and Hedrick (1996) proposed a control method using an input delay between control and response, but their results did not include the hydraulic dynamic processes and non-systematic input delay throttle and brake control. Gerdes (1996) and Gerdes and Hedrick (1995; 1997) introduced a sliding control to investigate brake delay based on the hydraulic dynamics of the master/slave

* Corresponding Author,
E-mail : kitchong@chonbuk.ac.kr
TEL : +82-652-270-2478; **FAX** : +82-652-270-2451
Faculty of Electronics and Information, Chonbuk National University, Duckjin-Dong, Duckjin-Gu, Chonju, 561-756, South Korea. (Manuscript **Received** September 20, 2005; **Revised** August 16, 2006)

cylinder, and presented their experimental results to verify the simulation of the integrated throttle and brake control processes.

In a retrofitted brake system, where the input force on the pushrod of the vacuum booster was used as the end control parameter, large simulation oscillation would occur because of the small desired input force was determined from the large diaphragm force and output force which have some uncertainties. Maciuca (1997) had used Fast Fourier Transform (FTT) smoothing to reduce the simulation oscillation. Maciuca and Hedrick (1995) also used an average estimated wheel pressure as the reference to reduce the simulation oscillation. Liang et al.(2003) used variable parameter sliding control with the pushrod force as the end control parameter, and introduced an average decay function to suppress both high and low frequency simulation oscillations.

Antilock brake systems (ABS) are closed-lop devices designed to prevent locking and skidding during braking (Austin and Morrey, 2000; Wellstead and Pettit, 1997; Unsal and Kachroo, 1999; Suh et al., 2002; Wu and Shih, 2003). Haskara et al.(2000) investigated wheel slip control for antispin acceleration via dynamic spark advance based on a typical tire force-relative slip curve, longitudinal motion dynamics of the vehicle and the dynamics of the wheel. Li et al.(2002) developed a vehicle electronic control system and its application to an ABS based o hardware-in-the-loop simulation, and the vehicle field test showed that the antilock brake deceleration reached about 9 m/s^2 on a high adhesion road condition. Since the typical ABS control the flow of high-pressure fluid between the master cylinder and the wheel caliper cylinder with high frequency pressure fluctuation features, an antilock brake control using the pushrod force as the end control parameter and the features are still the interesting topics.

In this paper, a 4-wheel vehicle model with tire slip effect was considered along with the variable parameter sliding control to investigate the vehicle longitudinal control performance. The variable sliding parameter is proportional to the square root of the pressure derivative at the wheel in order to compensate for large pressure change (Liang et al., 2003). A typical tire force-relative slip curve on dry road condition was used to fit out an analytical tire force-relative slip function, and an antilock sliding control process based the analytical tire force-relative slip function was used. A retrofitted brake system with the pushrod force as the end control parameter was employed, and an average decay function was used to suppress the simulation oscillations (Liang et al., 2003).

Section 2 presents the tire-force model and 4 wheels longitudinal state equations. The following section presents the sliding controllers for the brake process. Section 4 provides details on the upper sliding surface development for both speed and spacing control, adopting a switching logic proposed by Gerdes and Hedrick (1997). Section 5 describes the antilock control process. The simulation results to demonstrate the performance of the controller are presented in the Section 6, with conclusions finally being drawn in Section 7.

2. Longitudinal Vehicle Model

In this work a 4 wheels brake longitudinal vehicle model was used as shown in Figure 1. The 4 wheels of the vehicle were assumed to have identical parameters (wheel initial, tire force, brake pressure, etc) for the vehicle brake control processes. The wheel viscous friction force developed on the tire-road contact surface depends on the

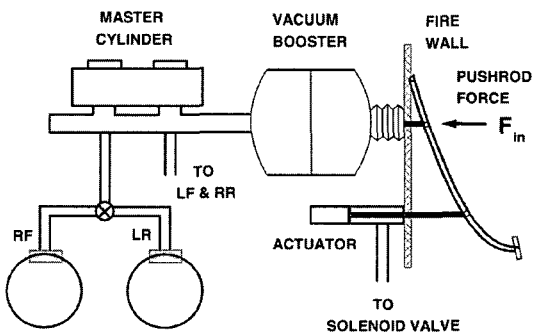

Fig. 1 Brake system diagram. The pushrod force F_{in} controls the out put force F_{out} from the vacuum booster, then F_{out} controls master cylinder pressure P_{mc} and slave cylinder pressure P_w

wheel slip σ, which was defined as the difference between the vehicle speed v, and the tire speed $\omega_w h$, normalized by the maximum of these velocity values (Unsal and Kachroo, 1999):

$$\sigma=\frac{\omega_w h-v}{\max(\omega_w h,\ v)} \tag{1}$$

where the wheel speed $\omega_w=R_g\omega_e$; h, R_g and ω_e are the tire radius, gear ratio and engine speed, respectively (Gerdes and Hedrick, 1995). The tire-road friction force on each wheel was determined by wheel slip, normal force, and tire-road adhesion coefficient μ. A typical tire force-relative slip curve F_{tire} on dry road condition was shown in Figure 2 (Haskara et al., 2000), which can be fitted using a simple function F_{fit} as shown in Fig. 2 (Yoshioka et al., 1999):

$$F_{fit}=a(1-e^{-b\sigma}-c\sigma) \tag{2}$$

where $a=5300$ N, $b=20$ and $c=0.264$ are the fitting parameters for dry road condition. The tire-road adhesion coefficient and tire force depend on road and tire conditions (Austin and Morrey, 2000). For the demonstration (simplicity) in the following simulation, a tire force-relative slip curve on snow road condition can be approximately selected for $0.25F_{fit}$ as shown in Fig. 2 (Haskara et al., 2000).

The longitudinal state equations can then be written by reflecting all of the forces and torques on the vehicle velocity v and the angular speed of each wheel ω_w (Gerdes and Hedrick, 1997; Unsal and Kachroo, 1999):

$$\dot{v}=\frac{R_g}{\beta}(4hF_w-M_{rr}-hF_a-F_g) \tag{3}$$

$$\dot{\omega}_w=\frac{1}{I_w}\left(\frac{\tau_e}{4R_g}-\tau_b-hF_w-\frac{M_{rr}}{4}\right) \tag{4}$$

where β is a lumped value combining the vehicle, engine, driveline and wheel inertia; τ_e and τ_b denote the engine torque and brake torque on each wheel; M_{rr} is the rolling resistance; $F_a=C_a v^2$ (C_a is an aerodynamic constant) and $F_g=mgh\sin\theta$ (θ is the road grade) are the aerodynamic drag and road grade forces, respectively (Gerdes and Hedrick, 1997); I_w is the wheel inertia; F_w is the tire force of each wheel, which can be calculated from Eq. (2) for the simulation (Unsal & Kachroo, 1999).

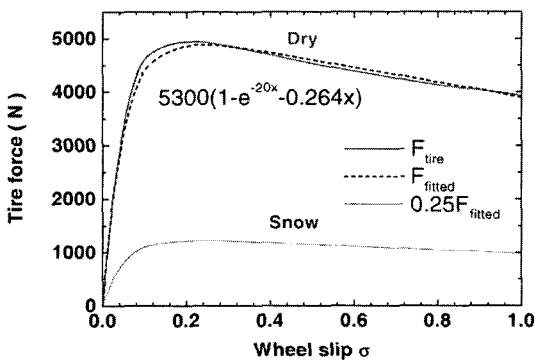

Fig. 2 A typical tire-relative slip curve on dry road F_{tire} (Haskara et al., 2000), the fitted tire-relative slip curve $F_{fitted}=5300\ (1-e^{-20x}-0.264x)$, and the selected tire-relative slip curve on snow road $0.25F_{fitted}$

3. Brake Control

3.1 Brake model

When the master cylinder pressure P_{mc} is used as the input to the brake system as shown in Fig. 1, the total brake torque of each wheel could be determined from the single-state model, in which the brake torque is proportional to the pressure at the wheel P_w through the gain K_b after a small "push-out" pressure P_{po} (Maciuca et al., 1994):

$$\tau_b=sign(P_w-P_{po})\,K_b(P_w-P_{po}) \tag{5}$$

Because of the compressive nature of the fluid and "push-out" pressure, the system exhibits time delays between the time the brake pressure is commanded at the master cylinder and the time this pressure is felt at the wheel.

The wheel pressure P_w is considered to be a function of the brake fluid volume V as shown in Figure 3. The fluid dynamics between the master (Fig. 1) and slave cylinders (close to the wheel not detailed in Fig. 1) is described by the following equation (Gerdes and Hedrick, 1997):

$$\dot{V}=sign(P_{mc}-P_w)\,C_q\sqrt{|P_{mc}-P_w|} \tag{6}$$

where C_q is a flow coefficient.

3.2 Variable parameter sliding control

Because measurement of wheel torque is pro-

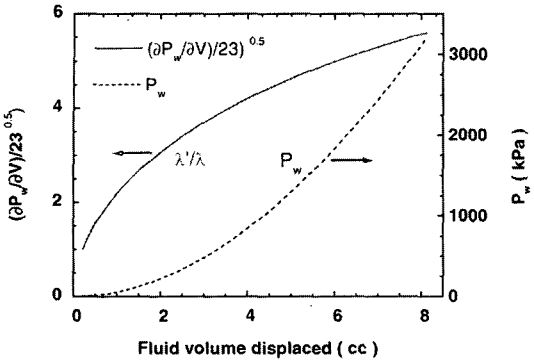

Fig. 3 The pressure at the wheel P_w, and the ratio of variable to constant sliding parameters $\lambda_b'/\lambda=\left(\frac{\partial P_w}{\partial V}/23\right)^{0.5}$ depend on fluid volume displacement

hibitively expensive at the present time, the control system using the signal, which comes from the wheel pressure. By translating the desired torque τ_{bd} into a desired wheel pressure P_{wd}, and assuming the hydraulic dynamics can be described by a first order nonlinear system, the sliding surface for brake control can be defined as $S_b=P_{wd}-P_w$ and $\dot{S}_b=-\lambda_b' S_b$. Substituting the actual dynamics into the sliding surface equations yields the sliding control equation (Gerdes and Hedrick, 1997):

$$\dot{P}_w=\dot{P}_{wd}-\lambda_b'(P_{wd}-P_w) \tag{7}$$

where

$$\dot{P}_w=sign(P_{mc}-P_w)\frac{\partial P_w}{\partial V}C_q\sqrt{|P_{mc}-P_w|} \tag{8}$$

The desired master cylinder pressure P_{mcd} for brake control can be deduced from Eqs. (7) and (8) as follows:

$$P_{mcd}=P_w+sign(\dot{P}_{wd}-\lambda_b'(P_w-P_{wd}))\left(\frac{\dot{P}_{wd}-\lambda_b'(P_w-P_{wd})}{\frac{\partial P_w}{\partial V}C_q}\right)^2 \tag{9}$$

where λ_b' is the variable sliding parameter (Liang et al., 2003):

$$\lambda_b'=\lambda_b\left(\frac{\frac{\partial P_w}{\partial V}}{\left(\frac{\partial P_w}{\partial V}\right)_b}\right)^{n_P} \tag{10}$$

where λ_b is the constant sliding parameter, the subscript "b" indicates a low limit reference point, at which $(\partial P_w/\partial V)_b=23$ and $V_b=0.22$ cc; n_P is the power index for the variable parameter of the sliding control. When $n_P=0$, $\lambda_b'=\lambda_b$, Eq. (10) reduces to constant sliding parameter. When $n_n=1$, λ_b' will compensate the factor of $\partial P_w/\partial V$ in Eq. (10) and lead to relatively uniform feedback in the entire braking range. By selecting $n_P=0.5$, λ_b'/λ_b will increase from 1 to 5.5, as V increases from 0.22 to 8 cc (see Fig. 3). The variable sliding parameter λ_b' (with $n_P=0.5$) will result in large brake control feedback and small tracking errors in the large V range, in comparison with $n_P=0$. Eq. (10) is expected to produce a faster response time in small V region in comparison with $n_P=0$. Thus $n_P=0.5$ allows λ_b' to partially compensate for the factor $\partial P_w/\partial V$ in Eq. (10), which in turn should result in relatively small brake control feedback and tracking errors, as well as better passenger comfort during the brake control process (Liang et al., 2003).

3.3 Pushrod force control

In the above sections, the control using master cylinder pressure as the end control parameter has been discussed, but this requires extensive redesign of the brake system (Gerdes, 1996). A retrofitted brake system with an actuator pulling on the brake pedal is by far the most straightforward design for applying the brake (Maciuca, Gerdes and Hedrick, 1994). When the pushrod force F_{in} is used as the end control parameter, the diaphragm force F_d will be controlled by F_{in}. The desired output force of the vacuum booster F_{outd} is determined from P_{mcd}. The desired input force F_{ind} can be calculated by (Gerdes, 1996):

$$F_{ind}=F_{outd}-F_{dd}+F_{rs} \tag{11}$$

where F_{rs} is the return spring force, and F_{dd} is the desired diaphragm force. The sliding surface for brake control can be defined as $S_{in}=F_{in}-F_{ind}$ and $\dot{S}_{in}=-\lambda_{in}S_{in}$. Substituting the actual dynamics yields the sliding control equation (Gerdes and Hedrick, 1997; Maciuca et al., 1994):

$$\dot{F}_{in}=\dot{F}_{in}-\lambda_{in}(F_{ind}-F_{in}) \tag{12}$$

Since F_{ind} is much smaller than F_{dd} and F_{outd}, the small uncertainty of F_{dd} and Foutd can result in significant oscillations of F_{ind} and F_{in}, generating

significant feedback oscillations in the simulation (Gerdes, 1996).

3.4 Average decay function for smoothing

In order to smooth the simulation results and estimate the control parameters, Fast Fourier Transform (FFT), Least-Squares Estimation, Least-Squares Estimation with Exponential Forgetting methods are used in the literature (Haskara et al., 2000; Huang and Ren, 1999; Maciuca, 1997). These standard integration-smoothing techniques are very powerful method of handling random data. However, the large oscillation of the parameter values in the simulation just switching between the maximum and minimum envelope curves with the envelope curves slowly changed. This feature indicates that the distribution of the data in the sliding control processes were not random. Therefore, none of these techniques produces the results desired for the switching oscillation data in the simulation. In this study, we found that averaging the two neighboring data values produces insignificant oscillations and the introduction of the exponential decay factor further smoothes the result. Therefore, an average decay function is used for the smoothing of parameters F_{outd}, F_{dd}, and F_w as follows (Liang et al., 2003):

$$A_{ad}(t)=A_{ad}(t-dt)+\left(\frac{A(t)+A(t-dt)}{2}-A_{ad}(t-dt)\right)\left(1-\exp\left(-\frac{dt}{\tau_s}\right)\right) \tag{13}$$

where d_t is the update interval for simulation, τ_s is the decay or response time constant of smoothing, and $A(t)$ and $A_{ad}(t)$ are the parameters before and after smoothing, respectively. Eq. (13) combines the average of the two neighboring data values with exponential decay smoothing to suppress the simulation oscillation. The selection of τ_s has little influence on the smoothing of fast oscillations, so it is set to the desired or actual system response time.

4. Speed and Spacing Control

4.1 Speed control

The objective of sliding control for speed tracking is to track the given desired velocity $v_d(t)$, defined by the sliding surface $S_v=v-v_d$. The system state is "driven" to this surface by $\dot{S}_v=-\lambda_u S_v$. The desired synthetic acceleration input for the lead car is obtained as follows (Gerdes and Hedrick, 1997):

$$a_{synth}=\dot{v}_d-\lambda_u(v-v_d) \tag{14}$$

4.2 Spacing control

For the spacing controller denoting the position, velocity and acceleration of the lead car by $x_l,\dot{x}_l,\ddot{x}_l$, respectively, and the corresponding quantities of the follower by $x_f,\dot{x}_f,\ddot{x}_f$, respectively, the spacing error ε is defined by (Gerdes and Hedrick, 1997)

$$\varepsilon=\Delta-(x_l-x_f) \tag{15}$$

where Δ is the desired spacing between the lead car and the following car. Defining the sliding surface by $S_u=\dot{\varepsilon}+\lambda_k\varepsilon$, the system state is "driven" to this surface by $\dot{S}_u=-\lambda_u S_u$, which yields the synthetic acceleration for the following car.

$$a_{synth}=\ddot{x}_l-\lambda_k\dot{\varepsilon}-\lambda_u(\dot{\varepsilon}+\lambda_k\varepsilon) \tag{16}$$

4.3 Switching between the throttle and brake

When the throttle is completely closed, the throttle characteristic is zero, but air continues to flow into the manifold through the throttle bypass, creating a minimum manifold pressure P_{ct} and closed throttle torque τ_{ct}. These parameters vary according to the engine speed and serve to define the lowest edge of the engine map (Gerdes, 1996). Therefore, engine torque τ_e can be divided into two parts: the closed-throttle-torque τ_{ct}, and the portion of the torque which is subject to control τ_{ec}. In the absence of control inputs, i.e. $\tau_e=\tau_{ct}$ and $\tau_b=0$ in Eq. (4), let $4hR_gF_w=\tau_{ct}$ in Eq. (3) and then, the residual acceleration, a_{resid}, can be defined as (Gerdes and Hedrick, 1997):

$$a_{resid}=\frac{1}{\beta}[\tau_{ct}-R_g(M_{rr}+hF_a+F_g)] \tag{17}$$

When the desired acceleration is greater than a_{resid}, a higher engine torque is required to accelerate the vehicle; otherwise, a brake torque is needed. By introducing a small hysteresis $\Phi=0.05$

m/s^2 to eliminate chatter, the switching criterion between throttle and brake is as follows:

$$\begin{aligned} &a_{synt} > a_{resid} + \Phi \Rightarrow \text{Throttle} \\ &a_{synt} < a_{resid} - \Phi \Rightarrow \text{Brake} \\ &a_{resid} + \Phi \geq a_{synt} \geq a_{resid} - \Phi \Rightarrow \text{Hold} \end{aligned} \tag{18}$$

Once the control action has been chosen, the desired engine torque for throttle or brake torque for the control will be:

$$\tau_{ed} = R_g (4 I_w \dot{\omega}_w + 4 h F_{wd} + M_{rr}) \tag{19}$$

$$\tau_{bd} = \frac{\tau_{ct}}{4 R_g} - \left(I_w \dot{\omega}_w + h F_{wd} + \frac{M_{rr}}{4} \right) \tag{20}$$

where the desired tire force F_{wd} was calculated form the synthetic acceleration:

$$F_{wd} = \frac{1}{4h} \left(\frac{\beta a_{synth}}{R_g} + M_{rr} + h F_a + F_g \right) \tag{21}$$

5. Antilock Control

From the tire force-relative slip Eq. (2), the critical slip value σ_c for the tire force reaches maximum F_{wc} can be solved as:

$$\sigma_c = \frac{1}{b} \ln \frac{b}{c} = 0.216 \tag{22}$$

$$F_{wc} = a \left(1 - \frac{c}{b} - \frac{c}{b} \ln \frac{b}{c} \right) = 4927\ N \tag{23}$$

The desired wheel acceleration $\dot{\omega}_{wcr}$ that corresponding to F_{wc} can be obtained from Eq. (4):

$$\dot{\omega}_{wcd} = \frac{1}{I_w} \left(\frac{\tau_e}{4 R_g} - \tau_b - h F_{wc} - \frac{M_{rr}}{4} \right) \tag{24}$$

When the wheel slip σ is larger than the critical slip σ_c, the tire force will decreases with increasing wheel slip, which would lead to the wheel to be locked. In order to draw the wheel slip towards to the critical slip σ_c to prevent the wheel to be locked, an antilock sliding control is introduced. The sliding surface for the antilock throttle or brake control can be defined as $S_s = \omega_{wc} - \omega_{wcd}$ and $\dot{S}_s = -\lambda_s (\sigma - \sigma_c) \omega_{wc}$. Substituting the actual dynamics yields the antilock sliding control equation:

$$\dot{\omega}_{wc} = \dot{\omega}_{wcd} - \lambda_c (\sigma - \sigma_c) \omega_{wc} \tag{25}$$

The desired engine torque or brake torque for the antilock sliding control will be:

$$\tau_{ed} = R_g (4 I_w \dot{\omega}_{wc} + 4 h F_w + M_{rr}) \tag{26}$$

$$\tau_{bd} = \frac{\tau_{ct}}{4 R_g} - \left(I_w \dot{\omega}_{wc} + h F_w + \frac{M_{rr}}{4} \right) \tag{27}$$

where the tire force F_w can be calculated from Eq. (2) with the wheel slip.

6. Simulation

The parameters used for simulation are similar to those used in Gerdes (1996) dissertation, along with a simulation step size of a 1 ms (update time), and with the transmission in third gear. The parameter values are shown in Table 1. The pushrod

Table 1 Parameter values used in the simulation

$dt = 1$ ms	$m = 2148$ kg
$\lambda_u = 1.5$	$\beta = 234$ kgm
$\lambda_k = 1$	$h = 0.33$ m
$\lambda_b = 10$	$M_{rr} = 72.6$ Nm
$\lambda_s = 10$	$C_a = 0.5334$ kg/m
$\lambda_{in} = 20$	$R_g = 0.326$
$\Phi = 0.05$ m/s^2	$C_q = 1.49$ cm^3/s
$MAX = 0.1834$ kg/m	$K_b = 0.81$
$V_m = 0.0027$ m^3	$P_{po} = 115$ kPa
$P_o = 10.67$ kPa	$V_a = 1.25$ cc
$A_{mc} = 4.9 \times 10^{-4}$ m^2	$P_a = 85$ kPa
$A_d = 0.0533$ m^2	$V_b = 0.22$ cc

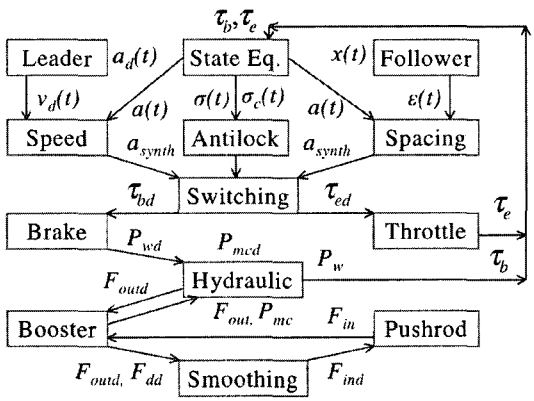

Fig. 4 Schematic diagram of brake and throttle simulation process

force, F_{in}, was used as the end control parameter. A block diagram of the simulation processes was shown in Figure 4.

The state Eqs. (3) and (4) were used to calculate the acceleration and speed of the cars and wheels, respectively. The wheel slip ratios and tire forces were calculated using Eqs. (1) and (2). The desired acceleration and speed of the lead car were obtained from Figure 5, combined with the speed controller defined in Eq. (14), in order to give the desired synthetic acceleration for the lead car. On the other hand, the spacing controller defined in Eq. (16), was used to calculate desired synthetic acceleration for the following car. The desired torque for throttle or brake and tire force can be calculated using Eqs. (19), (20) and (21), respectively. When the wheel slip ratio is larger than the critical slip σ_c, the desired antilock control torque for throttle or brake can be calculated using Eqs. (26) and (27). The desired master cylinder pressure P_{mcd}, was calculated from the sliding control, Eq. (9), and the force F_{outd}. The real-time diaphragm force F_d was calculated from the dynamics of the vacuum booster, and from the calculated value of the output force F_{out} and P_{mc}. However, the average decay function, which is defined in Eq. (13), was applied to F_{outd} and F_d, in order to evaluate F_{ind} using Eq. (11), and then F_{in} was determined by means of the sliding control Eq. (12). The torque parameters τ_b and τ_c, are fed back into the state Eqs. (3) and (4), for the simulation of the next update point. The simulation results, both for the small brake on a snow road, and large brake on a dry road, are shown in the Figs. (6)-(9) for comparison.

It can be seen in Figure 6(a) that both of the

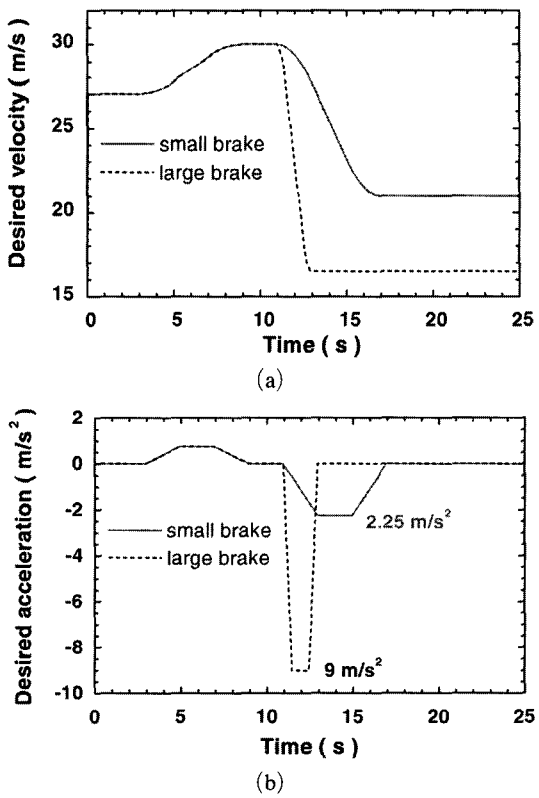

Fig. 5 The desired lead car velocity (a) and acceleration profiles (b) used in the simulation. The small and large brakes correspond to maximum 2.25 and 9.0 m/s^2 trapezoidal brake deceleration limits, respectively

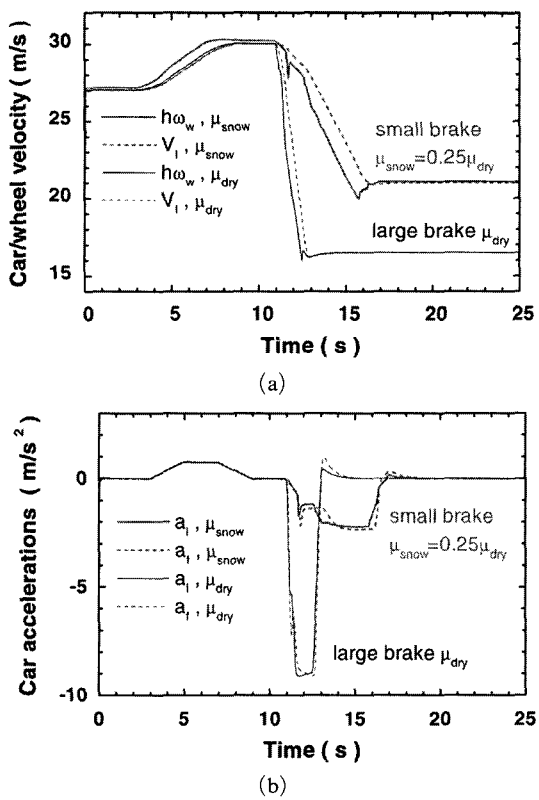

Fig. 6 Lead car velocity and wheel speed (a), lead car and following car accelerations (b) for small and large brake accelerations

wheel speed ($h\omega_w$) and car velocity (v_l) of the lead car are quite smooth in comparison with the simulation results (which show significant simulation fluctuations) in the case of ABS control (Li et al., 2002), because in the typical ABS control, a pulse-release pressure profile was used between master cylinder and wheel cylinder, which results in large pressure and wheel speed fluctuation. However, the push-rod force was used in this study, which results in certain system delay and relative smooth brake pressure (Liang et al., 2003). The wheel speed still shows some fluctuation when switching between throttle and brake, due to the small hysteresis, Φ=0.05 m/s^2, and system delay. Fig. 6(b) shows that the accelerations of the lead car (a_l) and following car (a_f) are fairly smooth, except for some fluctuations that occur when the switching between throttle and brake.

Figure 7(a) shows that the maximum speed tracking errors between the speeds of the lead car and the desired velocity ($v_l - v_d$) are 0.4 and 0.5 m/s for the large and small brake, respectively. The maximum spacing errors between the lead and the following cars are 0.35 and 0.4 m for the large and small brakes, respectively, as shown in Fig. 7(b). The spacing errors without considering slip effect are shown in Fig. 7(b) for comparison. It can be seen that the spacing errors that including slip effect are significantly larger than those of without considering slip effect at large brake (slip). The speed and spacing errors in the braking regions are much bigger than those in the throttle regions, for both the small and large brakes.

In order to show the wheel slip and tire force during the control process. The wheels slip (σ_l

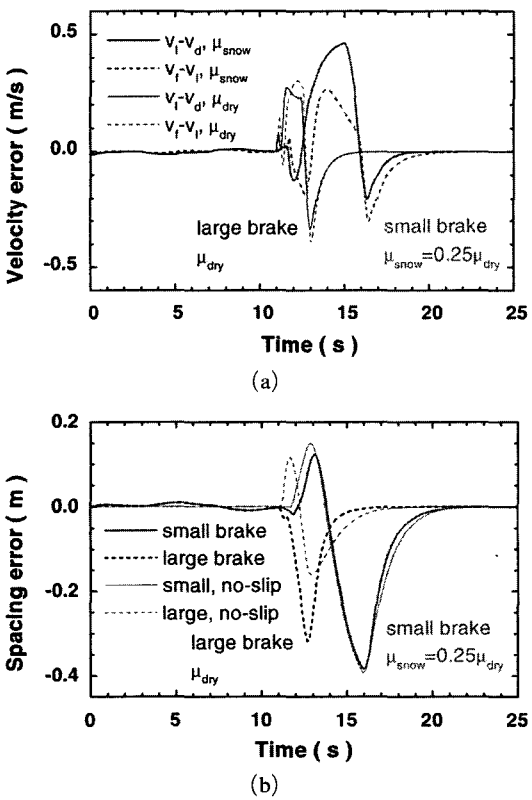

Fig. 7 The simulation tracking errors for small and large brake: (a) speed errors of the lead car and the follower, and (b) spacing errors between the lead car and the follower cars, the results that without wheel slip effect also shown for comparison

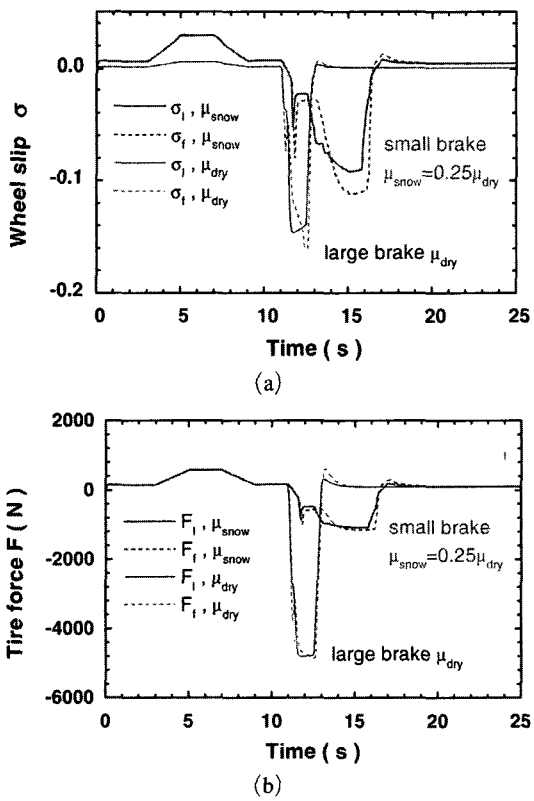

Fig. 8 The simulation wheel slip (a) and tire force of lead and follow cars (b)

and σ_f), and tire force (F_l and F_f) of the lead and following cars for both the small and large brakes are shown in Figure 8(a) and (b), respectively. The desired (P_{wd}) and actual (P_w) wheel brake pressures, and engine/brake torques (τ_{ed} and τ_{bc}) for both small and large brakes are shown in Figure 9(a) and (b).

Figure 10(a) and (b) show the maximum values (in the simulation time region from 0 to 25 s) of wheel slip and spacing errors of the lead and following cars depend on adhesion ratios for the small brake acceleration profile (as shown in Fig. 5). When the adhesion ratio (of the cars relative to the value on dry road condition), μ/μ_{dry}, is reduced from 1 to o.25, the maximum wheel slip changed slowly, while the maximum spacing errors remains almost unchanged, because the maximum wheel slip is smaller than the critical value, $\sigma_c \approx 0.2$. However, when μ/μ_{dry} further decreases from 0.25 to 0.19 (as shown in the insert), the maximum wheel slip rapidly increased to ~0.6 (larger than the critical value, $\sigma_c \approx 0.2$). The antilock control take action to prevent the wheel to be locked, while larger spacing error would be generated as the desired brake deceleration was larger than the brake deceleration provided by the antilock control process. The maximum spacing error for the lead car (relative to the desired position of the car) increased to ~3.5 m. The maximum spacing error for the following car first increased from 0.5 to 1.1 m, and then decreases to 0.5 m, due to the lead car experienced large wheel slip and spacing error. This is based on the supposition that adhesion ratio and wheel slip would not significantly increase the maximum spacing error for the control process used in this study, as long as the wheel slip is less than the critical value.

In order to demonstrate the effect on non-constant adhesion road condition (Pauwelussen et

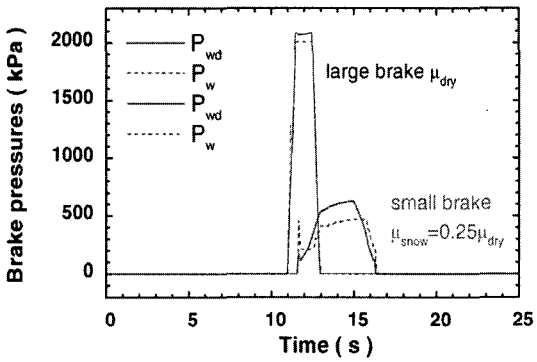

(a)

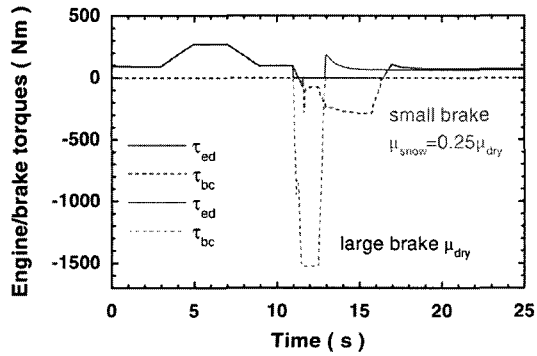

(b)

Fig. 9 The simulation brake pressure (a) and engine/brake torque of the lead car (b)

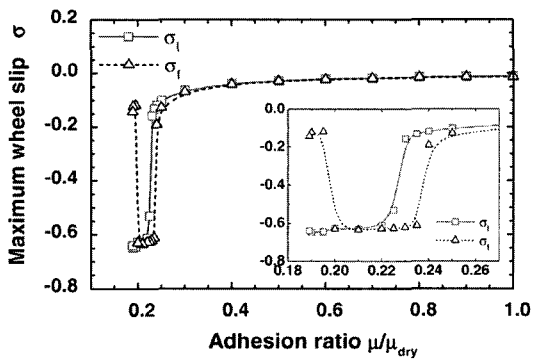

(a)

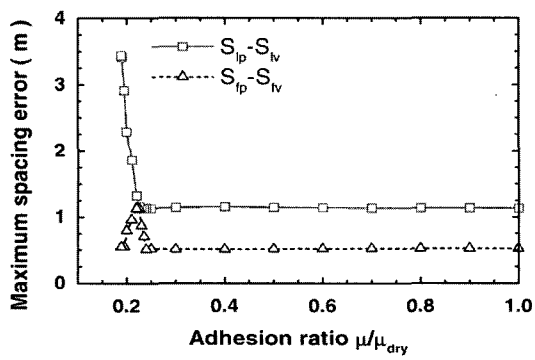

(b)

Fig. 10 The simulation wheel slip (a) and spacing errors (b) depend on adhesion ratio

al., 2003; Suh et al., 2002), an equivalent adhesion coefficient, $\mu_l=0.27\ (0.9+0.1\sin(5t))\,\mu_{dry}$, was used in the simulation (Ray, 1997; Ono et al., 2003). The simulation results of wheel slip and car/wheel velocity were shown in Fig. 11(a) and (b), respectively. It can be seen that the wheel slip and car/wheel velocity also oscillation corresponding to oscillation period of the effective adhesion coefficient. In some regions the wheel slip is larger than the critical value ($\sigma_c\approx0.2$) since the effective adhesion coefficient is smaller than the critical value on a dry road condition ($\mu_c\approx0.27\times0.8\mu_{dry}=0.21\mu_{dr}$), and the large wheel slip was controlled by the antilock slide control and the oscillation of adhesion. Therefore, to obtain the desired speed or spacing control profile, the acceleration limit for the wheel likely to become locked (or antilock control) was determined by the minimum adhesion of the oscillation.

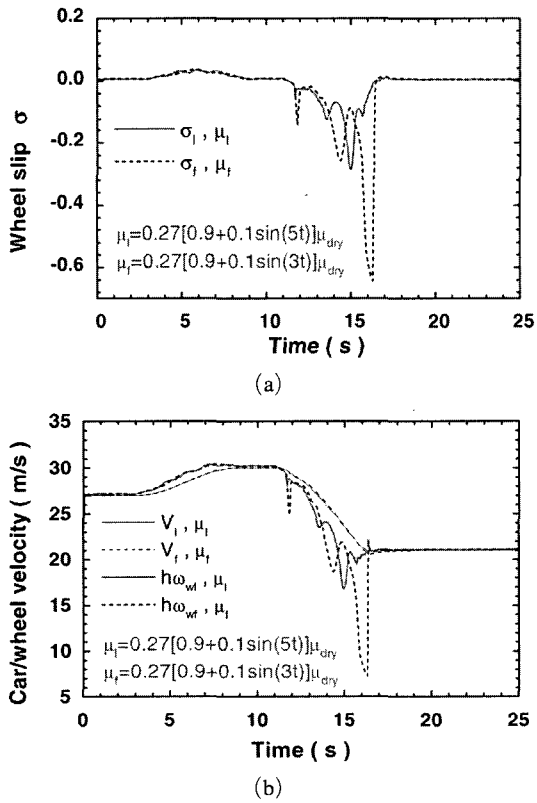

Fig. 11 The simulation wheel slip (a) and car/wheel velocity (b) depend on periodic oscillation slip coefficient on snow road

In other word, the wheel would easily become locked in either unstable adhesion or bumping road condition (oscillation of the tire force).

7. Conclusions

In this study, we investigated vehicle longitudinal brake control with wheel slip using the brake hydraulic dynamics of master/slave cylinders with variable sliding parameter $\lambda_b=\left(\frac{\partial Pw}{\partial V}\Big/\left(\frac{\partial P_w}{\partial V}\right)_b\right)^{0.5}$, the pushrod force as the end control parameter, and an antilock sliding control processes. The simulation results for both small and large brake profile show that the velocity and spacing errors in the brake region were slightly larger than those obtained in the case where wheel slip effect is not considered. The maximum spacing errors of the lead car and follower were insensitive to the adhesion ratios, provides that the wheel slip is less than the critical value. The acceleration limit for the antilock sliding control under non-constant adhesion road conditions was determined from the minimum of the equivalent adhesion coefficient. The antilock sliding control with pushrod force as the end control parameter, provides relative smooth wheel slip and car/wheel velocity, in comparison with the results of the typical ABS.

Acknowledgements

This work has been supported by the Regional Research Center for Mechatronics at Chonbuk National University, Korea. The authors would like to thank the Mechatronics Center at Chonbuk National University.

References

Austin, L. and Morrey, D., 2000, "Recent Advances in Antilock Braking Systems and Traction Control Systems," *Proceedings of the I MECH E Part D Journal of Automobile Engineering*, Vol. 214, No. 6, pp. 625~638.

Chien, C. C., Ioannou, P. and Lai, M. C., 1994, "Entrainment and Vehicle Following Controllers Design For Autonomous Intelligent Vehicles,"

Int Proc. ACC, pp. 6~11.

Choi, S. B. and Hedrick, J. K., 1996, "Robust Throttle Control of Automotive Engines : Theory and Experiments," *ASME J. DSMC 118*, pp. 92~98.

Gerdes, J. C. and Hedrick, J. K., 1995, "Brake System Requirements for Platooning on an Automated Highway," *In Proc. ACC*, pp. 165~169.

Gerdes, J. C. and Hedrick, J. K., 1997, "Vehicle Speed and Spacing Control Via Coordinated Throttle and Brake Actuation," *Control Engr. Practice*, Vol. 5, No. 11, pp. 1607~1614.

Gerdes, J. C., 1996, "Decoupled Design of Robust Controllers for Nonlinear Systmes : As Motivated by and Applied to Coordinated Throttle and Brake Control for Automated Highways," PhD dissertation. U.C. Berkeley, LA. CA.

Haskara, I., Özgüner, Ü. and Winkelman, J., 2000, "Wheel Slip Control for Antispin Acceleration Via Dynamic Spark Advance," *Control Eng. Practice*, Vol. 8, No. 10, pp. 1135~1148.

Huang, S. N. and Ren, W., 1999, "Vehicle Longitudinal Control using Throttles and Brakes," *Robotics and Autonomous Systems*, Vol. 26, No. 4, pp. 241~253.

Lee, K. J. and Park, K. H., 1999, "Optimal Robust Control of a Contactless Brake System Using an Eddy Current," *Mechatronics*, Vol. 9, No. 6, pp. 615~631.

Li, J., Yu, F., Zhang, J.W., Feng, J. Z. and Zhao, H. P., 2002, "The Rapid Development of a Vehicle Electronic Control System and its Application to an Antilock Braking System Based on Hardware-in-the-loop Simulation," *Proceedings of the I MECH E Part D Journal of Automobile Engineering*, Vol. 216, No. 2, pp. 95~105.

Liang, H., Chong, K. T., No, T. S. and Yi, S. Y., 2003, "Vehicle Longitudinal Brake Control Using Variable Parameter Sliding Control," *Control Engineering Practice*, Vol. 11, No. 4, pp. 403~411

Maciuca, D. B., Gerdes, J. C. and Hedrick, J. K., 1994, "Automatic Braking Control for IVHS," *Proceedings of the International Symposium on Advanced Vehicle Control (AVEC 1994), Tsukuba, Japan*, pp. 69~74

Maciuca, D. B., 1997, "Nonlinear Robust and Adaptive Control with Application to Brake Control for Automated Highway Systems," PhD dissertation, U.C. Berkeley, LA. CA.

Maciuca, D. B. and Hedrick, J. K., 1995, "Advanced Nonlinear Brake System Control for Vehicle Platooning," *Proceedings of the third European Control Conference (ECC 1995), Rome, Italy*.

Ono, E., Asano, K., Sugai, M., Ito, S., Yamamoto, M., Sawada, M. and Yasui, Y., 2003, "Estimation of Automotive Tire Force Characteristics Using Wheel Velocity," *Control Engineering Practice*, Vol. 11, No. 12, pp. 1361~1370.

Pauwelussen, J. P., Gootjes, L., Schröder, C., Köhne, K. -U., Jansen, S. and Schmeitz, A., 2003, "Full Vehicle ABS Braking Using the SWIFT Rigid Ring Tyre Model," *Control Engineering Practice*, Vol. 11, No. 2, pp. 199~207.

Ray, Laura R., 1997, "Nonlinear Tire Force Estimation and Road Friction Identification : Simulation and Experiments," *Automatica*, Vol. 33, No. 10, pp. 1819~1833.

Suh, M. W., Park, Y. K. and Kwon, S. J., 2002, "Braking Performance Simulation for a Tractor-semitrailer Vehicle with an air Brake System," *Proceedings of the I MECH E Part D Journal of Automobile Engineering*, Vol. 216, No. 1, pp. 43~54.

Swaroop D., 1994, "String Stability of Interconnected Applications to IVHS," PhD Dissertation, U.C. Berkeley, LA. CA.

Unsal, C. and Kachroo, P., 1999, "Sliding Mode Measurement Feedback Control for Antilock Braking Systems," *IEEE TRANSACTIONS ON CONTROL SYSTEMS TECHNOLOGY*, Vol. 7, No. 2, pp. 271~281.

Utkin, V. I., 1977, "Survey Paper, Variable Structure Systems with Sliding Modes," *IEEE Transactions on Automatic Control*, Vol. AC-22, No. 2, pp. 212~222.

Wellstead, P. E. and Pettit, N. B. O. L., 1997, "Analysis and Redesign of an Antilock Brake System Controller," *IEE PROCEEDINGS-CONTROL THEORY AND APPLICATIONS*, Vol. 144, No. 5, pp. 413~426.

Wu, M. C. and Shih, M. C., 2003, "Simulated and Experimental Study of Hydraulic Anti-lock

Braking System Using Sliding-mode PWM control," *Mechatronics*, Vol. 13, No. 4, pp. 331~351.

Yoshioka, T., Adachi, T., Butsuen, T., Okazaki, H. and Mochizuki, H., 1999, "Application of Sliding-mode theory to Direct Yaw-moment Control," *JSAE Review*, Vol. 20, No. 4, pp. 523~529